Catal Lett (2009) 130:130–136
DOI 10.1007/s10562-008-9798-5

Correlating Photoluminescence and Photocatalytic Activity of Mixed-phase Nanocrystalline Titania

K. V. Baiju · A. Zachariah · S. Shukla · S. Biju · M. L. P. Reddy · K. G. K. Warrier

Received: 6 October 2008 / Accepted: 21 November 2008 / Published online: 4 December 2008

Abstract Mixed-phase nanocrystalline titania with varying rutile-content has been synthesized via solvent mixing and calcination treatment of sol–gel derived nanocrystalline anatase and rutile precursors. The mixed-phase nanocrystalline titania has been characterized using different analytical techniques for analyzing their phase contents, nanocrystallite size distribution, band-gap, and photoluminescence. The photocatalytic activity of mixed-phase nanocrystalline titania has been studied by monitoring the degradation of methylene blue dye in an aqueous solution under ultraviolet-radiation exposure. A strong correlation between photoluminescence and photocatalytic activity has been demonstrated for the mixed-phase nanocrystalline titania.

Keywords Nanocrystalline · Photocatalytic activity · Photoluminescence · Sol–gel · Titania

1 Introduction

Photocatalysis is a low temperature non-energy intensive process for the chemical waste remediation and utilizes various wide band-gap semiconductor oxides including nanocrystalline titania (TiO_2). In this process, the electron (e^-) and hole (h^+) pairs are created by exposing photocatalyst particles to ultraviolet (UV) radiation having energy comparable with the band-gap of semiconductor oxide. They migrate to the surface producing surface-radicals such as hydroxyls (–$OH^\bullet$), atomic oxygen, and superoxide anions, which attack the surface-adsorbed dye molecules degrading them into various cations, anions, and gases [1–3].

The life-time of photon-induced e^-/h^+ pair, hence, plays a crucial role in determining the photocatalytic activity of nanocrystalline TiO_2. Different parameters have been demonstrated in the literature, which affect the life-time of photo-induced e^-/h^+ pair, such as the average nanocrystallite size [4], dopants [4–6], noble-metal surface-catalyst [7, 8], foreign surface-oxide [9, 10], and amount of rutile [11]. As summarized in detail by others [4], it has been demonstrated that for these systems, variation in the photo-induced e^-/h^+ life-time can be qualitatively studied via photoluminescence (PL) analysis, which can be then correlated with the photocatalytic activity of semiconductor oxides. However, such correlation between PL and photocatalytic activity has not been reported for the nanocrystalline TiO_2 having different weight-fractions of mixed anatase and rutile phases. The synergy effect between the anatase and rutile phases of mixed-phase nanocrystalline TiO_2 is known to enhance the photocatalytic activity of pure anatase-TiO_2 [12]. Hence, establishing the correlation between PL and photocatalytic activity of mixed-phase nanocrystalline TiO_2 is of significance, which is currently lacking in the literature.

From this point of view, in the present investigation, we synthesize mixed-phase nanocrystalline TiO_2 with varying rutile-content, via sol–gel solvent mixing and calcination

K. V. Baiju · A. Zachariah · S. Shukla (✉) · K. G. K. Warrier
Ceramic Technology Department, Materials and Minerals Division (MMD), National Institute for Interdisciplinary Science and Technology (NIIST), Council of Scientific and Industrial Research (CSIR), Industrial Estate P.O., Pappanamcode, Thiruvananthapuram, Kerala 695019, India
e-mail: satyajit_shukla@csrrltrd.ren.nic.in

S. Biju · M. L. P. Reddy
Chemical Sciences and Technologies Division (CSTD), National Institute for Interdisciplinary Science and Technology (NIIST), Council of Scientific and Industrial Research (CSIR), Industrial Estate P.O., Pappanamcode, Thiruvananthapuram, Kerala 695019, India

(SMC) and demonstrate that variation in the photocatalytic activity as a function of amount of rutile is strongly related to the photo-induced e^-/h^+ life-time estimated qualitatively via PL analysis.

2 Experimental

2.1 Chemicals

Titanium(IV)-isopropoxide ($Ti[OC_3H_7]_4$) and anhydrous 2-propanol were purchased from Alfa Aesar, India; and methylene blue (MB) (AR Grade) from Qualigens Fine Chemicals, India. All chemicals were used as-received without any further purification.

2.2 Sol–Gel Processing of Mixed-phase Nanocrystalline TiO_2

In order to synthesize the mixed-phase nanocrystalline TiO_2, amorphous-TiO_2 was first processed via sol–gel using the '*R*' (ratio of molar concentration of water and to that of alkoxide-precursor) value of 90, as described in detail elsewhere [13, 14]. A part of dried amorphous powder was then calcined at 400 °C for 1 h to crystallize into the anatase-TiO_2 and remaining powder was calcined at higher temperature, 800 °C for 2 h, to crystallize completely into rutile-TiO_2. The calcination at 400 °C for 1 h was selected just to nucleate anatse-TiO_2 nanocrystals in the amorphous-TiO_2 matrix. This ensured that, during the final calcination at 600 °C for 2 h, the amorphous-TiO_2 is transformed only to anatase-TiO_2.

Anatase-TiO_2 and rutile-TiO_2 were then utilized as precursors to obtain the nano-composites of two phases, with different rutile-content, via SMC process. In this technique, rutile-TiO_2 precursor was first physically mixed, using a mortar and pestle, in different weight-ratios (5, 20, 40, 60, and 100 wt%) with anatase-TiO_2 precursor. The physically mixed precursors were then dispersed, under continuous magnetic stirring for 1 h, in 100 mL of anhydrous 2-propanol to achieve homogenous mixing. The suspension was then dried in an oven at 80 °C till the solvent was evaporated completely. The nanocrystalline TiO_2, with homogeneously mixed anatase-TiO_2 and rutile-TiO_2 precursors, was then calcined at 600 °C for 2 h for establishing an electronic coupling between the two phases. In our earlier investigation [13], it was demonstrated that, for the present sol–gel method involving $Ti[OC_3H_7]_4$ precursor, the anatase-TiO_2 is stable up to 600 °C above which it gets transformed to rutile-TiO_2. Hence, to avoid the anatase-to-rutile phase transformation and improve the crystallinity, the highest temperature of 600 °C was selected for the final calcination.

2.3 Characterization of Mixed-phase Nanocrystalline TiO_2 Processed Via Sol–Gel-SMC

The transmission electron microscope (TEM, Tecnai G^2, FEI, Netherlands) images of nanocrystalline TiO_2 powders processed under different conditions were obtained at 300 kV to obtain the average nanocrystallite size and its distribution. The selected-area electron diffraction (SAED) patterns were obtained to confirm the nano-crystallinity and nature of phases involved.

The crystalline phases present in the mixed-phase nanocrystalline TiO_2 were determined using X-ray diffraction (XRD, Rigaku, Japan). The broad-scan analysis was conducted within *2-θ* range of 10–80° using Cu Kα (λ_{Cu} = 1.542 Å) radiation. The obtained XRD patterns were then utilized to determine the weight-fraction of rutile-TiO_2 using the equation,

$$\text{Rutile-TiO}_2\ (\text{wt\%}) = \frac{I_{(110)R} \times 100}{I_{(110)R} + (0.8)I_{(101)A}} \quad (1)$$

where, I_A and I_R represent the linear-intensities of main-peaks of anatase-TiO_2 $(101)_A$ and rutile-TiO_2 $(110)_R$.

The absorption spectra of mixed-phase nanocrystalline TiO_2, with different rutile-content, were obtained using ultraviolet-visible (UV-vis) spectrophotometer (UV-2401 PC, Shimadzu, Japan), operated in the diffuse reflectance (DR) mode, for wavelength within the range of 200–800 nm. The band-gap was calculated using the equation,

$$\text{Band-gap} = \frac{hc}{\lambda_{int}} \quad (2)$$

where, '*h*' is the Plank's constant (4.135×10^{-15} eV s), '*c*' the velocity of light (3×10^8 m s^{-1}), and 'λ_{int}' the wavelength (m) corresponding to the intersection of extension of linear-part of the spectrum and x-axis.

The PL spectra, obtained at an excitation wavelength of 327 nm, were recorded on a Spex-Fluorolog FL22 spectrofluorometer equipped with a double grating 0.22 m Spex 1680 monochromator and a 450 W Xe Lamp as an excitation source operating in the front face mode.

2.4 Photocatalytic Activity of Mixed-phase Nanocrystalline TiO_2 Processed Via Sol–Gel-SMC

The photocatalytic activity of mixed-phase nanocrystalline TiO_2, processed via sol–gel-SMC, was studied by monitoring the degradation of MB dye in an aqueous suspension containing the mixed-phase nanocrystalline TiO_2 under continuous UV-radiation exposure and magnetic stirring. A 75 mL of aqueous suspension was prepared by completely dissolving 0.0064 μmol L^{-1} of MB dye and then dispersing 0.4 g L^{-1} of mixed-phase nanocrystalline TiO_2 in the de-ionized water. The resulting suspension was

equilibrated by stirring in dark (without UV-radiation exposure) for 1 h to stabilize the adsorption of MB dye on the surface of nanocrystalline TiO_2.

The stable aqueous suspension was then exposed to UV-radiation, with continuous magnetic stirring, using Rayonet Photoreactor (The Netherlands) containing 15 W tubes (Philips G15 T8) as the UV-source, which emitted the UV-radiation having wavelength within the range of 200–400 nm (corresponding to the photon energy range of 3.07–6.14 eV). Following UV-radiation exposure, 3 mL of aqueous suspension was taken out of UV-chamber after each 10 min interval for total 1 h of UV-radiation exposure for obtaining the absorption spectra.

The nanocrystalline TiO_2 was filtered out from the sample suspension using a centrifuge (R23, Remi Instruments India Ltd.) and filtered solution was examined using a UV-vis spectrophotometer to study the degradation of MB dye. The absorption spectra of MB dye solution were obtained within the range of 200–800 nm as a function of UV-radiation exposure time for the mixed-phase nanocrystalline TiO_2 with different rutile-content. The intensity of main absorption peak (A) of MB dye solution, located at 656 nm, was taken as a measure of residual MB dye concentration (C). The UV-vis absorption spectrum of MB dye solution (A_o), without the addition of nanocrystalline TiO_2 and UV-radiation exposure, was also recorded as a reference spectrum corresponding to initial MB dye concentration (C_o). The normalized residual MB dye concentration was calculated using relationship of the form,

$$\left(\frac{C}{C_0}\right)_{\mathrm{MB}} = \left(\frac{A}{A_0}\right)_{656\mathrm{nm}} \tag{3}$$

A photocatalysis experiment was also performed in the absence of nanocrystalline TiO_2 photocatalyst to confirm the stability of MB dye in an aqueous solution under continuous UV-radiation exposure. Under this condition, the initial MB dye concentration (C_o) remained unchanged even after irradiating the sample for total 1.5 h.

3 Results and Discussion

The TEM images of sol–gel derived anatase-TiO_2 and rutile-TiO_2 precursors have been presented in Figs. 1a and 1b; while, that of mixed-phase nanocrystalline TiO_2 with 40 wt% rutile has been presented in Fig. 1c. The anatase-TiO_2 precursor, Fig. 1a, is noted to consist of aggregated nanocrystallites within the size range of ~5–15 nm. The corresponding SAED pattern, shown as an inset in Fig. 1a, displays continuous rings suggesting the nanocrystalline nature of anatase-TiO_2 precursor. The rutile-TiO_2 precursor, Fig. 1b, also consists of aggregated nanocrystallites; however, the nanocrystallite size is observed to be much larger within the range of ~50–150 nm. As a result, the corresponding SAED pattern shown as an inset in Fig. 1b is observed to be spotty. The mixed-phase nanocrystalline TiO_2 with 40 wt% rutile, Fig. 1c, shows the presence of both anatase-TiO_2 and rutile-TiO_2 phases and the corresponding SAED pattern (see the inset) consists of both the continuous rings as well spots. Moreover, the two phases are in contact with each other, which suggests the development of an electronic coupling in between them, which is the most essential requirement for the observed correlation between PL and photocatalytic activity of mixed-phase nanocrystalline TiO_2 processed via sol–gel-SMC.

Typical broad-scan XRD patterns obtained using the mixed-phase nanocrystalline TiO_2 with rutile-content of 20 and 40 wt% are presented in Fig. 2. The anatase-TiO_2 and rutile-TiO_2 are identified by comparing the spectra with the JCPDS files # 21–1272 and # 21–1276. It is clearly seen that, with increasing addition of rutile-TiO_2 during sol–gel-SMC, the intensity of main-peak of rutile-TiO_2 in the XRD spectra also increases. Using Equation 1, the weight-fractions of rutile-TiO_2 are calculated to be 25 and 37 wt% respectively, which are comparable with those considered during the processing of mixed-phase nanocrystalline TiO_2.

Typical absorption spectra obtained for the mixed-phase nanocrystalline TiO_2 with 5, 40, and 60 wt% rutile are presented in Fig. 3. The powders with 5 and 40 wt% rutile show absorption in the UV-region below 400 nm. Due to larger amount of rutile content, which has smaller band-gap than that of anatase-TiO_2, the powder with 40 wt% rutile shows higher absorption near the visible-region relative to that of powder with 5 wt% rutile as indicated by the presence of shoulder in the spectra near the visible-region. Using Equation 2, the band-gap of these two powders has been estimated to be 3.37 eV, which is larger than 3.2 eV corresponding to that of bulk anatase-TiO_2. An enhancement in the band-gap is attributed to the small nanocrystallite size range of ~5–15 nm, which is less than the critical size (~17 nm) required for the band-gap enhancement [15]. For the powder with 60 wt% rutile, the band-gap is calculated to be 3.28 eV which is smaller than that of other two powders and the absorption near the visible-region is also seen to be enhanced due to higher rutile-content. The band-gap of pure rutile-TiO_2 has been estimated to be 3.06 nm, which is comparable with the bulk-value.

The PL spectra of mixed-phase nanocrystalline TiO_2 with varying rutile-content, obtained at an excitation wavelength of 327 nm, are presented in Fig. 4. It is noted that, all the powders show a broad PL peaking at 486 nm in the visible-region, which is an excitonic PL attributed to defects present in the samples, namely the oxygen-ion vacancies, which provide acceptor levels near the

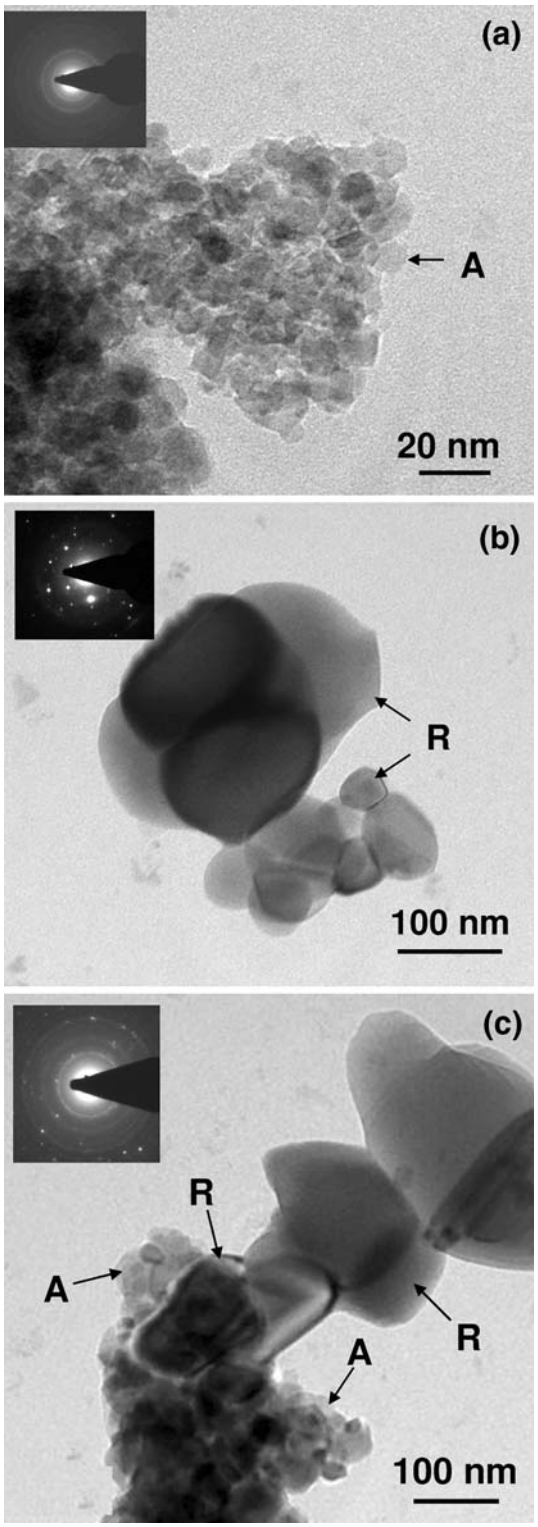

Fig. 1 Typical TEM images of sol–gel derived anatase-TiO_2 (**a**), rutile-TiO_2 (**b**) precursors and mixed-phase nanocrystalline TiO_2 with 40 wt% rutile processed via sol–gel-SMC (**c**). Insets show corresponding SAED pattern. '*A*' and '*R*' represent anatase-TiO_2 and rutile-TiO_2

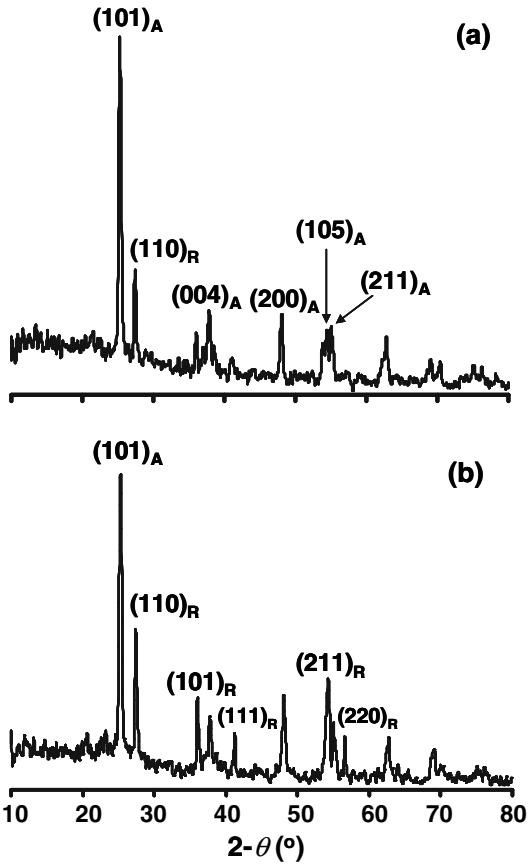

Fig. 2 Typical broad-scan XRD patterns obtained for the mixed-phase nanocrystalline TiO_2 processed via sol–gel-SMC with the rutile-content of 20 (**a**) and 40 (**b**) wt%. '*A*' and '*R*' represent anatase-TiO_2 and rutile-TiO_2

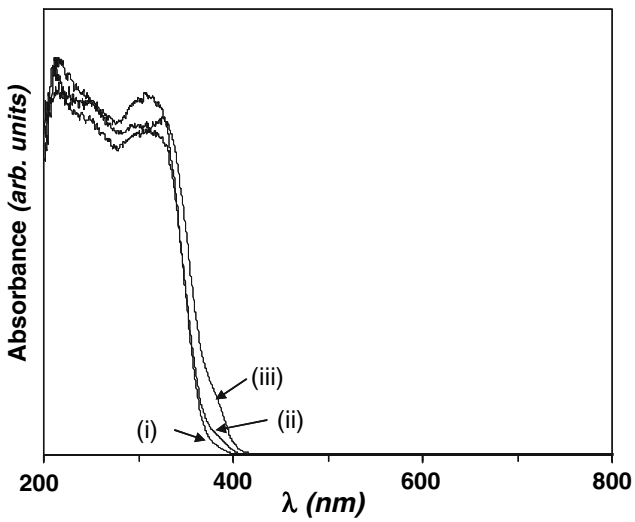

Fig. 3 Typical absorption spectra obtained for the mixed-phase nanocrystalline TiO_2 with 5 (i), 40 (ii), and 60 (iii) wt% rutile

conduction-band edge, and hence, mediate the transfer of photo-induced electrons from the conduction-band to valence-band [4]. In Fig. 4a, the PL intensity is seen to decrease progressively (as indicated by an arrow) as the amount of rutile increases within the range of 5–40 wt%. However, as observed in Fig. 4b, the PL intensity increases (as indicated by an arrow) with the amount of rutile within the range of 40–100 wt%. Thus, the trend in variation of PL intensity of mixed-phase nanocrystalline TiO_2 as a function of amount of rutile is different below and above 40 wt% rutile. Since all the powders have been produced in pure form under the similar processing conditions, variation in the PL intensity can not be attributed to the changes in the oxygen-ion vacancy concentration in different powders. However, such variation can be very well explained using the charge-separation mechanism [16] and a newly proposed model based on variation in the band-gap of mixed-phase nanocrystalline TiO_2 as a function of size-distribution and phases involved [17].

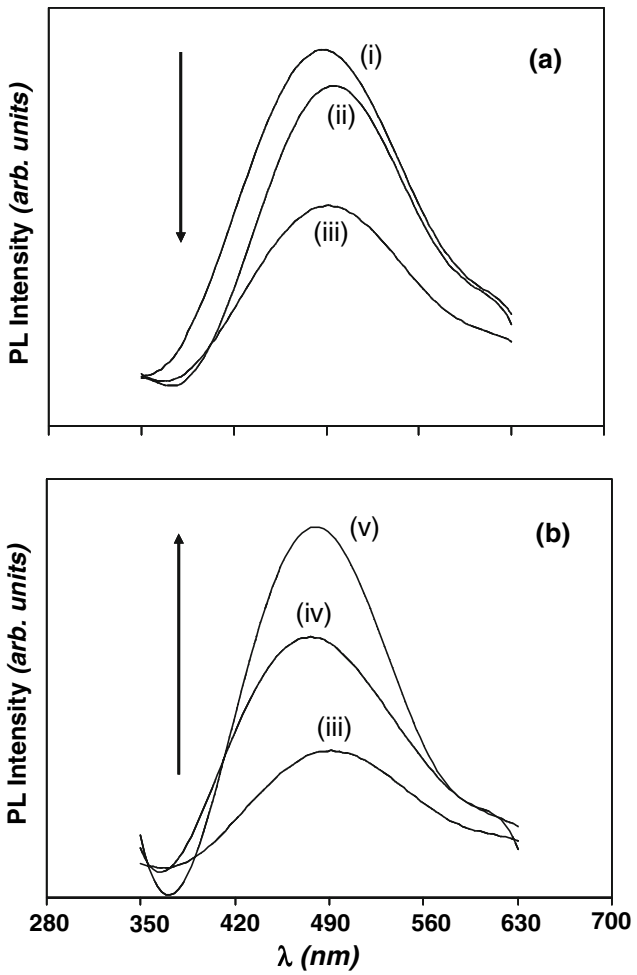

Fig. 4 Typical PL spectra obtained for the mixed-phase nanocrystalline TiO_2 for the rutile-content within the range of 5–40 wt% (**a**) and 40–100 wt% (**b**). In **a** and **b**, (i–v) correspond to 5, 20, 40, 60, and 100 wt% rutile respectively. Excitation wavelength used is 327 nm

According to these mechanisms, when the anatase-TiO_2 and rutile-TiO_2 are in contact with each other, Fig. 1c, the photo-induced holes in anatase-TiO_2 accumulate in rutile-TiO_2; while, the photo-induced electrons remain in anatase-TiO_2 due to band bending at the interface. This results in an effective charge-separation and increased photo-induced e^-/h^+ life-time. The PL intensity is, hence, expected to reduce for the mixed-phase nanocrystalline TiO_2 having the anatase-TiO_2 and rutile-TiO_2 in electronic contact with each other. As a consequence, the decreasing PL intensity as observed in Fig. 4a is attributed to an increased number anatase-rutile contacts with increasing rutile-content within the range of 5–40 wt%.

However, for higher amount of rutile above 40 wt%, more rutile-rutile contacts are established, which dominate the anatase-rutile contacts. Since former contacts are not as effective as latter contacts for an effective charge-separation, the photo-induced e^-/h^+ life-time decreases with increasing rutile-content within the range of 40–100 wt%.; which in turn increases the PL intensity within this range. Thus, the PL analysis suggests the maximum photo-induced e^-/h^+ life-time for the mixed-phase nanocrystalline TiO_2 with 40 wt% rutile.

Variation in the normalized residual MB concentration as a function of UV-radiation exposure time is shown in Fig. 5a; while, the corresponding plots for obtaining an apparent first-order reaction rate-constant (k_{app}) have been presented in Fig. 5b. The obtained variation in k_{app} as a function of amount of rutile is shown Fig. 6. It is seen that, k_{app} increases with increasing rutile-content and reaches a maximum value at 40 wt% rutile. It is well known that, the degradation of MB in an aqueous solution under UV-radiation exposure, in the presence of nanocrystalline TiO_2 photocatalyst, takes place via the formation (using photo-induced e^-/h^+ pairs) and successive attacks of $OH^\bullet$-radicals [13]. Under present processing conditions, the concentration of $OH^\bullet$-radicals formed is dependent on the life-time of photo-induced e^-/h^+ pairs. Higher the photo-induced e^-/h^+ life-time, higher would be the concentration of $OH^\bullet$-radicals and the degradation rate of MB. Hence, the maximum photocatalytic activity observed at 40 wt% rutile, Fig. 6, suggests that the photo-induced e^-/h^+ life-time is maximum for this powder, which is in accord with the PL analysis. Thus, a strong correlation between the PL and photocatalytic activity of mixed-phase nanocrystalline TiO_2 processed via sol–gel-SMC is observed.

It is to be noted that, Martinez et al. [18] recently conducted the photocatalysis experiments in a gaseous medium, and observed that, the photocatalytic activity of mixed-phase nanocrystalline TiO_2 increases with increasing anatase-to-rutile weight-ratio as a result of increased

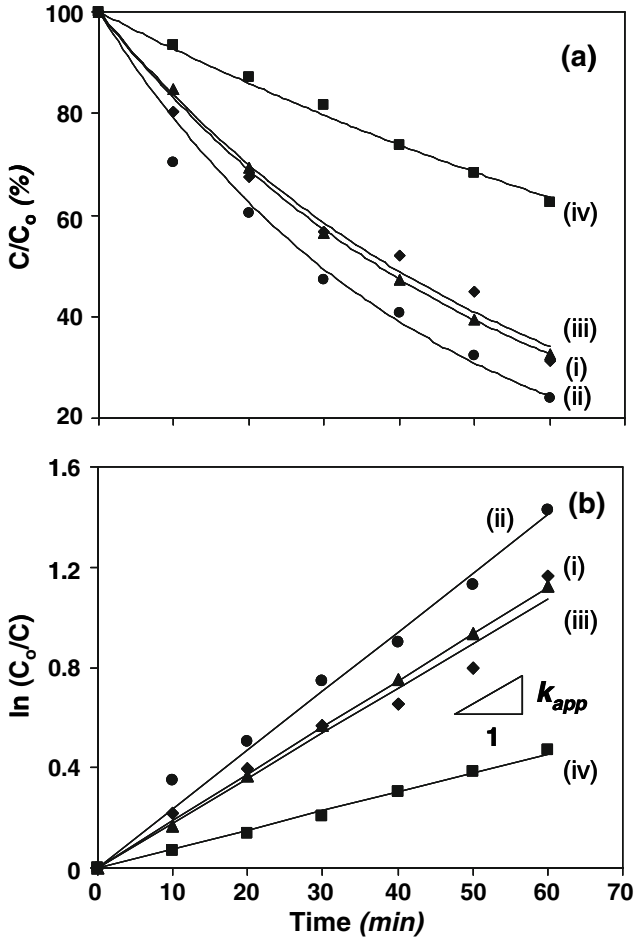

Fig. 5 Typical variation in the normalized residual MB concentration as a function of UV-exposure time (**a**) and the corresponding plots for determining k_{app} for the mixed-phase nanocrystalline TiO_2 processed via sol–gel-SMC. In **a** and **b**, (i–iv) correspond to 5, 40, 60, and 100 wt% rutile respectively

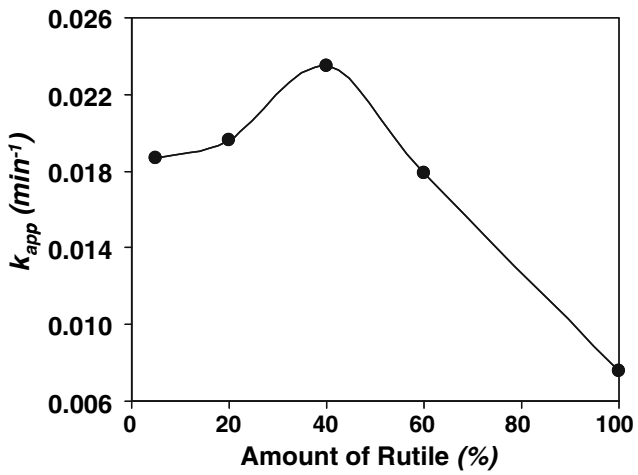

Fig. 6 Variation in k_{app} as a function of amount of rutile as derived from the plots presented in Fig. 5b

amount of surface-adsorbed water from the gaseous surrounding. In the present investigation, however, since the photocatalytic activity has been measured in an aqueous solution, the amount of surface-adsorbed water is not dependent on the anatase-to-rutile weight-ratio. Hence, observed variation in the photocatalytic activity can not be explained here on the basis of amount of surface-adsorbed water as suggested by Martinez et al. [18]. On contrary, this has been satisfactorily explained based on variation in the electronic interaction between the involved phases as a function of rutile-content, which is also reflected in the similar variation in the PL intensity.

4 Conclusions

The mixed-phase nanocrystalline TiO_2 with varying rutile-content has been synthesized via sol–gel-SMC. Variation in the photocatalytic activity of mixed-phase nanocrystalline TiO_2 as a function of amount of rutile is shown to be related to the variation in photo-induced e^-/h^+ life-time as estimated qualitatively via PL analysis. Hence, there appears to be a strong correlation between the PL and photocatalytic activity of mixed-phase nanocrystalline TiO_2 processed via sol–gel-SMC.

Acknowledgements Authors thank the Department of Science and Technology (DST), India (Project # GAP 205139), and the Council of Scientific and Industrial Research (CSIR), India (Network Project # NWP0010 and Task Force Project # CMM0019) for funding the ceramic, nanotechnology, and photocatalysis research at NIIST-CSIR. Authors also thank Mr. P. Mukundan (NIIST-CSIR, India), and Mr. Narendra (Icon Analytical, India) for conducting the DR and TEM analyses.

References

1. Houas A, Lachheb H, Ksibi M, Elaloui E, Guillard C, Herrmann J-M (2001) Appl Catal B 31:145
2. Zhao L, Yu Y, Song L, Hu X, Larbot A (2005) Appl Surf Sci 239:285
3. Fujishima A, Rao TN, Tryk DA (2000) J Photchem Photobiol C 1:1
4. Liqiang J, Yichun Q, Baiqi W, Shudan L, Baojiang J, Libin Y, Wei F, Honggang F, Jiazhong S (2006) Sol Energy Mater Sol Cells 90:1773
5. Jing LQ, Sun XJ, Xin BF, Cai WM, Fu HG (2004) J Solid State Chem 177:3375
6. Li XZ, Li FB, Yang CL, Ge WK (2001) J Photochem Photobio A 141:209
7. Kuo Y-L, Chen H-W, Ku Y (2007) Thin Solid Films 515:3461
8. Li FB, Li XZ (2002) Appl Catal A 228:15
9. Shang J, Yao WQ, Zhu YF, Wu N (2004) Appl Catal A 257:25
10. Korosi L, Papp S, Ménesi J, Illes E, Zollmer V, Richardt A, Dekany I (2008) Colloids Surf A 319:136
11. Kolen'ko YV, Churagulov BR, Kunst M, Mazerolles L, Justin CC (2004) Appl Catal B 54:51

12. Yan M, Chen F, Zhang J, Anpo M (2005) J Phys Chem B 109:8673
13. Baiju KV, Shukla S, Sandhya KS, James J, Warrier KGK (2007) J Phys Chem C 111:7612
14. Baiju KV, Shukla S, Sandhya KS, James J, Warrier KGK (2008) J Sol-Gel Sci Technol 45:165
15. Lin H, Huang CP, Li W, Ni C, Shah SI, Tseng Y-H (2006) Appl Catal B 68:1
16. Sun B, Vorontsov AV, Smirniotis PG (2003) Langmuir 19:3151
17. Zachariah A, Baiju KV, Shukla S, Deepa KS, James J, Warrier KGK (2008) J Phys Chem C 112:11345
18. Martınez VC, Ortiz AL, Elguezabal AA (2007) Int J Chem Reactor Eng 5:A92